

Supporting Information

Relay-Like Exchange Mechanism through a Spin Radical between TbPc₂ Molecules and Graphene/Ni(111) Substrates

Simone Marocchi,^{†,⊥} Andrea Candini,[†] David Klar,[‡] Willem Van den Heuvel,[¶] Haibei Huang,[¶] Filippo Troiani,[†] Valdis Corradini,[†] Roberto Biagi,^{†,#} Valentina De Renzi,^{†,#} Svetlana Klyatskaya,[§] Kurt Kummer,^{||} Nicholas B. Brookes,^{||} Mario Ruben,^{§,@} Heiko Wende,[‡] Umberto del Pennino,^{†,#} Alessandro Soncini,[¶] Marco Affronte,^{†,#} and Valerio Bellini[†]

[†]S3 - Istituto di Nanoscienze - CNR, Via Campi 213/A, 41125 Modena, Italy; [⊥]Universidade de São Paulo-IFSC Av. Trabalhadores são-carlense, 400, São Carlos, Brazil; [‡]Faculty of Physics and Center for Nanointegration Duisburg-Essen (CENIDE), University of Duisburg-Essen, Lotharstrasse 1, D-47048 Duisburg, Germany; [¶]School of Chemistry, University of Melbourne, VIC 3010, Australia; [#]Dipartimento di Scienze Fisiche, Matematiche e Informatiche, Università di Modena e Reggio Emilia, Via Campi 213/A, 41125 Modena, Italy; [§]Institute of Nanotechnology, Karlsruhe Institute of Technology (KIT), D-76344 Eggenstein-Leopoldshafen, Germany; ^{||}European Synchrotron Radiation Facility (ESRF), Avenue des Martyrs 71, 38043 Grenoble, France; [@]Institut de Physique et Chimie des Materiaux de Strasbourg, UMR 7504 Uds-CNRS, 67034 Strasbourg Cedex 2, France.

DFT calculation of TbPc₂ on top-bridge stacked graphene/Ni(111) substrates

The results presented in the main text for the top-fcc stacking of graphene/Ni(111) hold also in the case of top-bridge stacking, and a similar difference of tens of meV between the AFM and FM

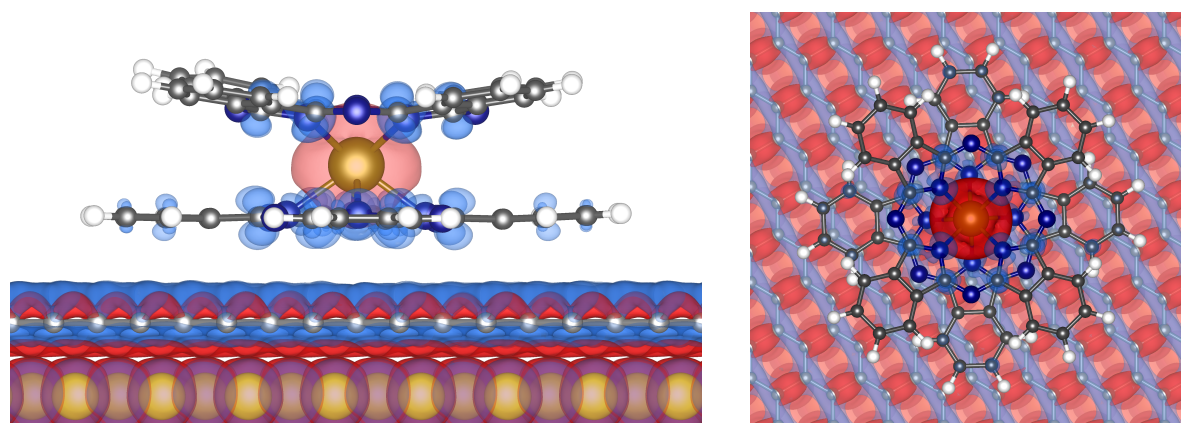


Figure S1: Side (left panel) and top (right panel) view of the spin-polarized charge density isosurfaces of TbPc₂ molecule adsorbed on top-bridge stacked graphene/Ni(111); blue (red) color stands for spin up (down) spin-polarization, relative to the positive (up) Ni magnetization.

coupling of the radical with the Ni slab is observed. In Figures S1 and S2 the spin density at the

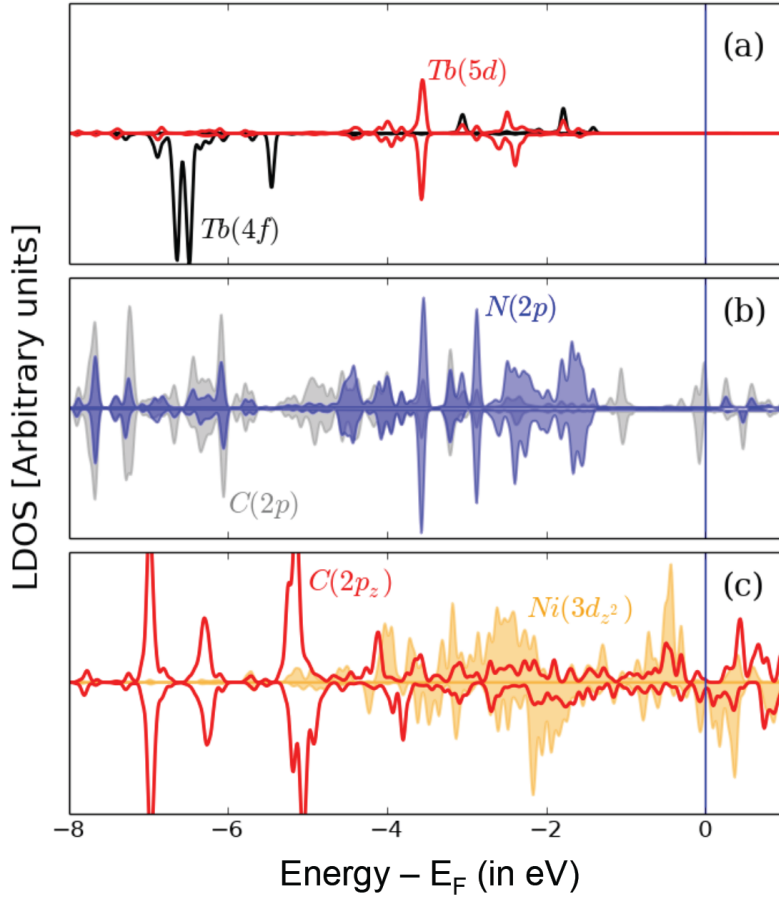


Figure S2: Spin-polarized LDOS of TbPc₂ on graphene/Ni(111) in the top-bridge stacking for the ground state configuration. (a) 4*f* and 5*d* states of Tb of TbPc₂; (b) the projections on the 2*p* orbitals of the nearest-neighbours to the Tb ion, N and C atoms, enlarged atoms in the sketch of Fig. 5 in main article; (c) 3*d*_{*z*²} states of the first layer of Ni and 2*p*_{*z*} states of C equivalent atoms in the bridge-top configuration. The *d* states of the Ni layer are plotted in orange, while graphene C *p*_{*z*} states are in red. In each panel, the upper (lower) side is relative to the majority (minority) spin channel. The DOS of *d*-character in panels (a) has been enhanced for better comparison.

molecule-substrate interface region and the LDOS are presented, respectively.

Implementation of the spin model Hamiltonian for the multi-domain magnetic structure of Ni single crystal

Differently from Ref. S1, where Ni films were deposited either on Cu(100) or Ag(100), our choice to use a Ni(111) single crystal presses us to devise a model which takes into account the multi-domain magnetic structure of the substrate.

We approximate the total Ni magnetization to be given by the sum of the magnetizations of two different type of domains, in which the Ni spins are either fully aligned along (“up” domains) or opposite to (“dn” domains) the applied external magnetic field.

Within each domain the magnetization is constant, and set either to +1 or -1. In absence of the external field, the abundance of each kind of domains balances out, and the net Ni magnetization is zero. When a magnetic field is applied, there is an unbalance between the two kind of domains, the ones aligned towards the external field increase in number and size, up to when the macroscopic saturation field is reached and only one type of domain exists, i.e. the Ni magnetization reaches its maximum value. Since the size of magnetic domains is usually much larger than the size of a single molecule, we suppose each molecule to be adsorbed on top of a graphene region, which, in turn, is on top of either one of the two types of Ni domains, and the molecule(radical)-Ni coupling being well approximated by an effective isotropic exchange term.

Following the above assumptions, Equation 1 in the text could be split and rewritten as

$$\begin{aligned}
 H_{\text{up}} &= H_{\text{CF}} + \mu_B(\hat{\mathbf{L}} + 2\hat{\mathbf{S}} + 2\hat{\mathbf{s}}) \cdot \mathbf{B} \\
 &\quad + J_{\text{exch}}\hat{\mathbf{S}} \cdot \hat{\mathbf{s}} + \frac{K}{|B|}\hat{\mathbf{s}} \cdot \mathbf{B}, \\
 H_{\text{dn}} &= H_{\text{CF}} + \mu_B(\hat{\mathbf{L}} + 2\hat{\mathbf{S}} + 2\hat{\mathbf{s}}) \cdot \mathbf{B} \\
 &\quad + J_{\text{exch}}\hat{\mathbf{S}} \cdot \hat{\mathbf{s}} - \frac{K}{|B|}\hat{\mathbf{s}} \cdot \mathbf{B},
 \end{aligned}
 \tag{S1}$$

where the (+) or (-) sign in the last term depends on whether the molecule is adsorbed on an “up” or “dn” type domain, i.e. the magnetization of each Ni domain has been set either to +1 or -1.

The two Hamiltonians are then solved independently in the usual way, obtaining eigenvalues and eigenvectors, and calculating the operators’ expectation values separately, performing the usual statistical sum over the states populated at a specific temperature.

In this way, the equilibrium Tb magnetizations, at that temperature, of a molecule on top of the “up” and “dn” domains, i.e. $M_{\text{up}}^{\text{Tb}}(B)$ and $M_{\text{dn}}^{\text{Tb}}(B)$ are obtained independently from each other.

Finally, we use the experimental Ni magnetization curve as a function of the external field to calculate the relative weights of the two magnetizations, i.e. w_{up} and w_{dn} at each applied field B,

$$\begin{aligned}
 w_{\text{up}}(B) &= [1 + M_{\text{Ni}}(B)]/2 \\
 w_{\text{dn}}(B) &= [1 - M_{\text{Ni}}(B)]/2
 \end{aligned}
 \tag{S2}$$

and use them to recover the total Tb magnetization $M_{\text{tot}}^{\text{Tb}}(B)$, as the weighted sum of the magnetizations extracted by Eqs. S1, i.e.

$$M_{\text{tot}}^{\text{Tb}}(B) = w_{\text{up}}(B) * M_{\text{up}}^{\text{Tb}}(B) + w_{\text{dn}}(B) * M_{\text{dn}}^{\text{Tb}}(B) \quad \text{S3}$$

Approximated spin-model Hamiltonian following CASSCF calculations

The Hamiltonian in Eq. 1 in the main text acts in the space of the $J=6$ spin-orbit multiplet of Tb^{3+} coupled to the $s=1/2$ of the radical. The CASSCF calculations predict a degenerate $|M_J=\pm 6\rangle$ ground doublet, separated by about 300 cm^{-1} from the excited states, so that an appropriate reduced Hilbert space to model the magnetization consists of the four states $|M_J=\pm 6\rangle |m_s=\pm 1/2\rangle$.

The Hamiltonian reduces in this space to

$$\begin{aligned} H_{\text{up}} &= J_{\text{exch}}g_S\hat{J}_z\hat{S}_z + \mu_B g_J B \cos \Theta \hat{J}_z \\ &\quad + (2\mu_B B + K)(\cos \Theta \hat{S}_z + \sin \Theta \hat{S}_x) \\ H_{\text{dn}} &= J_{\text{exch}}g_S\hat{J}_z\hat{S}_z + \mu_B g_J B \cos \Theta \hat{J}_z \\ &\quad + (2\mu_B B - K)(\cos \Theta \hat{S}_z + \sin \Theta \hat{S}_x) \end{aligned} \quad \text{S4}$$

with $g_J=3/2$ and $g_S=1/2$.

We have assumed the magnetic field in the xz plane, at an angle θ with the z axis. To obtain the magnetization of Tb along the direction of the applied field we calculate the thermal average of $\hat{J}_z \cos \theta$ for both Hamiltonians separately, and then take the weighted average according to Eq. S3 above. Finally a proportionality factor is applied to account for the arbitrary units of the XMCD signal.

XPS characterization of the TbPc₂ film

We have investigated the chemical composition of the TbPc₂ molecules deposited on the graphene/Ni(111) surface by means of X-ray photoemission spectroscopy (XPS). Figure S3 shows the core levels of the TbPc₂/graphene/Ni(111) system for two different molecular coverage.

Core level intensities have been analyzed taking into account the atomic sensitivity and the attenuation of the electronic signals. The $\text{N-1s}/\text{Tb-3d} = 18 \pm 5$ ratio is well reproducible and close to the expected one, i.e. 16, indicating that the molecular stoichiometry is preserved during the sublimation process. From the $\text{Tb-3d}/\text{Ni-2p}$ ratio and by taking into account the Ni signal attenuation due to the graphene overlayer, we obtained the average area occupied by one TbPc₂ molecule. Considering an area of $\sim 2 \text{ nm}^2$ for each molecule and assuming that the coverage is made

by molecules all lying flat on the surface, a thickness of 0.4-0.6 ML for the TbPc₂ film is derived, in agreement with the estimation made using the quartz microbalance.

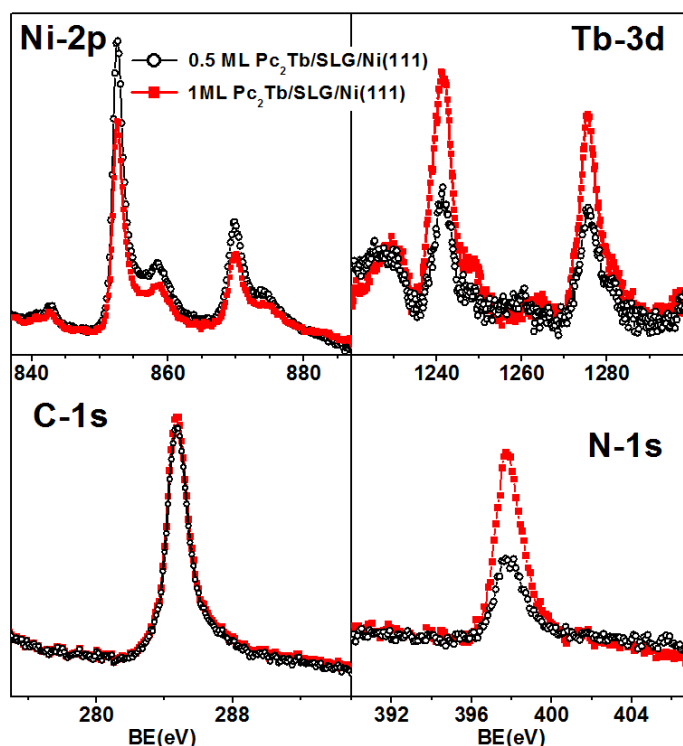


Figure S3: XPS core levels for the TbPc₂ deposited by sublimation on the graphene/Ni(111) surface for two different coverages (0.5ML and 1ML).

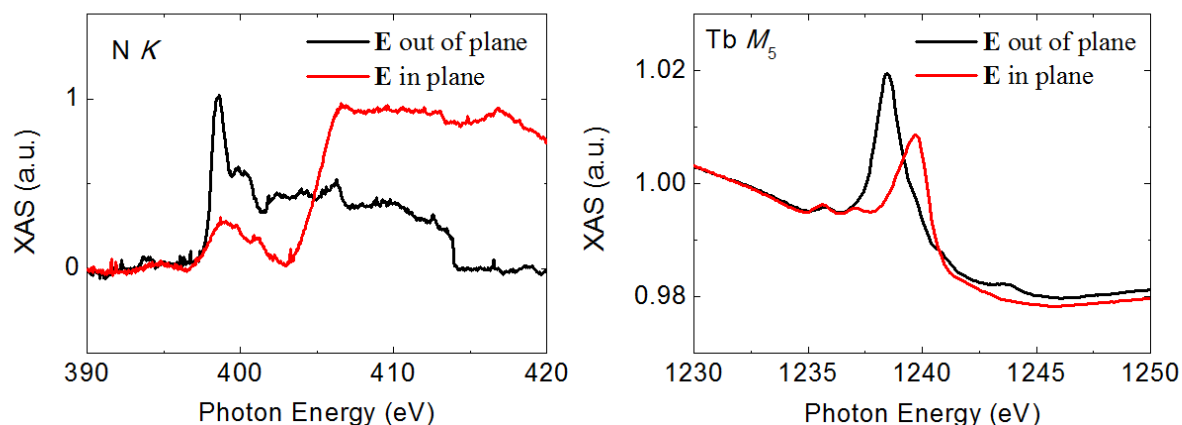


Figure S4: X-ray linear dichroism at the (left) N *K* edge and (right) Tb *M*₅ edge.

X-ray Linear Dichroism characterization of the TbPc₂ film

In Fig. S4 we present the X-ray Linear Dichroism (XLD) on the N *K* and Tb *M*_{4,5} edges which are found in agreement with what reported in previous works where TbPc₂^{S2,S3,S4} and metal-Pc^{S5,S6} were deposited on substrates, showing that the TbPc₂ molecules are flat on the substrate, with the Pc plane parallel to the surface.

XAS and XMCD spectra and magnetization cycle of the Ni(111) substrate

In Fig. S5 we show the XAS and XMCD spectra for the Ni $L_{2,3}$ edge in the TbPc₂/graphene/Ni(111)

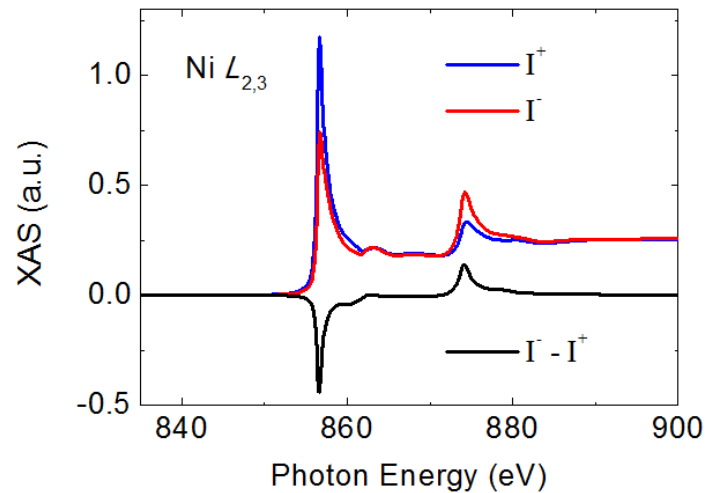


Figure S5: XAS and XMCD spectra for the Ni $L_{2,3}$ edge with an external field of 4T.

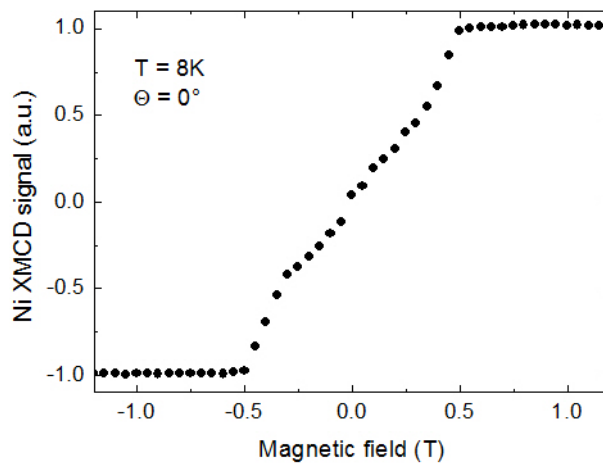


Figure S6: XMCD magnetization for the Ni(111) substrate taken at $\theta=0^\circ$. The magnetization is saturated for magnetic fields higher than ± 0.5 T.

system taken with an external applied field of 4 T. The Ni signal is found to be isotropic. In Fig. S6 the XMCD magnetization for the Ni(111) substrate taken at $\theta=0^\circ$ is displayed.

References

^{S1} Lodi Rizzini, A.; Krull, C.; Balashov, T.; Kavich, J. J.; Mugarza, A.; Miedema, P. S.; Thakur, P. K.; Sessi, V.; Klyatskaya, S.; Ruben, M.; Stepanow, S.; Gambardella, P. Coupling Single Molecule Magnets to Ferromagnetic Substrates. *Phys. Rev. Lett.* **2011**, *107*, 177205.

- ^{S2} Stepanow, S.; Honolka, J.; Gambardella, P.; Vitali, L.; Abdurakhmanova, N.; Tseng, T.- C.; Rauschenbach, S.; Tait, S. L.; Sessi, V.; Klyatskaya, S.; Ruben, M.; Kern, K. Spin and Orbital Magnetic Moment Anisotropies of Monodispersed Bis(Phthalocyaninato)Terbium on a Copper Surface. *J. Am. Chem. Soc.* **2010**, *132*, 11900–11901.
- ^{S3} Margheriti, L.; Chiappe, D.; Mannini, M.; Car, P.-E.; Sainctavit, P.; Arrio, M.- A.; de Mongeot, F. B.; Cezar, J. C.; Piras, F. M.; Magnani, A.; Otero, E.; Caneschi, A.; Sessoli, R. X-Ray Detected Magnetic Hysteresis of Thermally Evaporated Terbium Double-Decker Oriented Films. *Adv. Mater.* **2010**, *22*, 5488–5493.
- ^{S4} Biagi, R.; Fernandez-Rodriguez, J.; Gonidec, M.; Mirone, A.; Corradini, V.; Moro, F.; De Renzi, V.; del Pennino, U.; Cezar, J. C.; Amabilino, D. B.; Veciana, J. X-ray Absorption and Magnetic Circular Dichroism Investigation of Bis(Phthalocyaninato)Terbium Single-Molecule Magnets Deposited on Graphite. *Phys. Rev. B* **2010**, *82*, 224406.
- ^{S5} Wende, H.; Bernien, M.; Luo, J.; Sorg, C.; Ponpandian, N.; Kurde, J.; Miguel, J.; Piantek, M.; Xu, X.; Eckhold, Ph.; Kuch, W.; Baberschke, K.; Panchmatia, P. M.; Sanyal, B.; Oppeneer, P. M.; Eriksson, O. Substrate-Induced Magnetic Ordering and Switching of Iron Porphyrin Molecules *Nat. Mater.* **2007**, *6*; 516.
- ^{S6} Bernien, M.; Miguel, J.; Weis, C.; Ali, Md. E.; Kurde, J.; Krumme, B.; Panchmatia, P. M.; Sanyal, B.; Piantek, M.; Srivastava, P.; Baberschke, K.; Oppeneer, P. M.; Eriksson, O.; Kuch, W.; Wende, H. Tailoring the Nature of Magnetic Coupling of Fe-Porphyrin Molecules to Ferromagnetic Substrates. *Phys. Rev. Lett.* **2009**, *102*, 047202.